ELSEVIER

Ceramics International 29 (2003) 815–819

CERAMICS INTERNATIONAL

www.elsevier.com/locate/ceramint

Dielectric properties of $Pb[(Mg_zZn_{1-z})_{1/3}(Ta, Nb)_{2/3}]O_3$ ceramics ($z = 0.4,0.6$)

Seung-Mo Lim, Min-Chul Chae, Nam-Kyoung Kim*, Byung-Ok Park

Department of Inorganic Materials Engineering, Kyungpook National University, Daegu 702-701, South Korea

Received 23 September 2002; received in revised form 12 December 2002; accepted 20 January 2003

Abstract

In an attempt to stabilize a perovskite structure in $Pb(Zn_{1/3}Ta_{2/3})O_3$, Mg (40 and 60 at.%) and Nb (full composition range) were simultaneously substituted for Zn and Ta, respectively. B-site precursor compositions were synthesized separately, followed by PbO addition, in order to promote perovskite formation, whose content has been determined by X-ray diffraction. Low-frequency dielectric responses of the ceramic system were investigated under weak-field conditions. Effects of substituent concentration on the perovskite formation and dielectric properties are discussed.

Keywords: A. Powders: solid-state reaction; B. X-ray methods; C. Dielectric properties; D. Perovskites; Precursors

1. Introduction

It is well known that perovskite development in certain $A(B',B'')O_3$ compositions by conventional solid-state-calcination methods is quite difficult due to the formation of unwanted pyrochlore phase(s), the presence of which (even in small quantities in the perovskite matrices) is reported to be detrimental to dielectric properties [1,2]. $Pb(Zn_{1/3}Nb_{2/3})O_3$ (PZN) is a typical example, where perovskite formation has been realized only under very high pressure [3], via mechanochemical reaction routes [4], or by the aid of fluxes during crystal growth [5,6]. Meanwhile, the ferroelectric relaxor $Pb(Mg_{1/3}Nb_{2/3})O_3$ (PMN) and $Pb(Mg_{1/3}Ta_{2/3})O_3$ (PMT) of a perovskite structure have been successfully prepared via a two-step calcination route. The method [separate reactions among the B-site components for $(B',B'')O_2$-type precursors, followed by post-reactions of the product with PbO for $Pb(B',B'')O_3$ formation] has been proven to be highly effective in the synthesis of complex-perovskite compositions by ingeniously bypassing the pyrochlore formation route [7,8]. Nevertheless, perovskite $Pb(Zn_{1/3}Ta_{2/3})O_3$ [PZT, which in the present paper does not stand for $Pb(Zr,Ti)O_3$, but for a tantalum-analog of PZN] has not been synthesized by any means (including the B-site precursor method) so far [2,9–12].

Tantalum and niobium are representative pentavalent cations and frequently incorporated into the octahedral B″ site of a complex-perovskite lattice, e.g., $Pb(B^{+}_{1/4}B''_{3/4})O_3$, $Pb(B^{2+}_{1/3}B''_{2/3})O_3$, and $Pb(B^{3+}_{1/2}B''_{1/2})O_3$. Between the two ions, Nb is known to be more active in the perovskite development. Meanwhile, it was reported [13] that only a pyrochlore structure was detected at the whole compositions in a binary system of PZT–PZN, i.e., $Pb(Zn_{1/3}(Ta, Nb)_{2/3}]O_3$. In addition, replacements of Zn by more-ionic Mg of 20 at.% somewhat promoted the perovskite formation (especially at PZN-rich compositions), but the amount (20 at.%) turned out to be still insufficient to fully stabilize the perovskite in the entire system compositions. In the present study, therefore, further replacements by Mg (40 and 60 at.%), along with partial/full substitutions of isovalent Nb for Ta, were attempted in order to increase the perovskite phase contents at PZT-rich compositions as well. In this regard, the B-site precursor method was used to suppress the formation of parasitic pyrochlore(s), thereby improving dielectric characteristics.

* Corresponding author. Tel.: +82-53-950-5636; fax: +82-53-950-5645.

E-mail address: nkkim@knu.ac.kr (N.-K. Kim).

0272-8842/03/$30.00
doi:10.1016/S0272-8842(03)00021-X

2. Experimental

Nominal compositions of the two systems under investigation are $Pb[(Mg_{0.6}Zn_{0.4})_{1/3}(Ta_{1-x}Nb_x)_{2/3}]O_3$ and $Pb[(Mg_{0.4}Zn_{0.6})_{1/3}(Ta_{1-y}Nb_y)_{2/3}]O_3$, which will be referred to as systems I and II, respectively. The values of x and y (concentrations of substituent Nb) were changed from 0.0 to 1.0 at regular intervals of 0.2. The raw materials used were oxide chemicals of high purity (>99.5%). In order to maintain stoichiometries as closely to the nominal values as possible, moisture contents of the raw chemicals and of the separately-prepared precursor powders were measured and introduced into the batch calculations.

B-site precursors of the two systems were prepared from stoichiometric powder mixtures by wet-milling, drying, and calcination at 1100–1150 °C (depending on compositions) for 2 h in air. The lumps were then milled, dried, and calcined again under the same conditions to promote phase development. After PbO addition to the precursor powders (also in stoichiometric proportions), the mixtures were calcined at 850 and 950–1050 °C for 2 h each in both systems, with intermediate milling and drying steps for phase development. Calcined powders were examined by X-ray diffraction (XRD) to identify the phases formed. After the addition of 2 wt.% polyvinyl alcohol as a binder, the powders were pressed isostatically into pellets. The preforms were then fired at 1100–1250 °C for 2 h in a multiple-enclosure crucible setup [14] in order to suppress lead loss during exposure to elevated temperatures. Sintered ceramic samples were ground/polished to attain parallel surfaces, over which Au was sputtered for electrical contacts. Weak-field (~1 V_{rms}/mm) low-frequency (1, 10, 100, and 1000 kHz) dielectric constant values were measured over a temperature range of −140–180 °C on cooling.

3. Results and discussion

Developed structures in the B-site precursor systems of $(Mg_{0.6}Zn_{0.4})(Ta_{1-x}Nb_x)_2O_6$ and $(Mg_{0.4}Zn_{0.6})(Ta_{1-y}Nb_y)_2O_6$ are reported in Fig. 1(a) and (b), respectively. The XRD pattern of $x=0.0$ (i.e., $(Mg_{0.6}Zn_{0.4})Ta_2O_6$) matched that of the trirutile structure ($MgTa_2O_6$, ICDD #32-631), indicating that 40 mol% component of $ZnTa_2O_6$ (tri-αPbO_2 structure, ICDD #39-1484) had been completely dissolved into the host solid solution. At $x=0.2$, however, the trirutile was immediately replaced by columbite as the major phase, along with a negligible amount of tri-αPbO_2. Intensities of the trirutile structure decreased even further at $x=0.4$ and finally disappeared at $0.6\leqslant x$, leaving only the reflections of columbite. By careful inspection of the diffraction intensities (e.g., $2\theta=38.0°$, 53.4°, etc.) of $x=1.0$ (i.e., $(Mg_{0.6}Zn_{0.4})Nb_2O_6$), the spectrum was much closer to that of $MgNb_2O_6$ (columbite structure, ICDD #33-875), rather than that of $ZnNb_2O_6$ (columbite structure, ICDD #37-1371), even though they formed a continuous solid solution [15].

Similarly, a trirutile structure was the major one identified at $y=0.0$ of $(Mg_{0.4}Zn_{0.6})Ta_2O_6$, together with a small amount of tri-αPbO_2, indicating that most of the $ZnTa_2O_6$ component (60 mol%) had assimilated to the host structure of trirutile solid solution. The reflections of the trirutile, however, virtually disappeared at $y=0.2$ and became undetectable at $0.4\leqslant y$. Meanwhile, the tri-αPbO_2 structure was predominant at $y=0.2$, yet almost disappeared at $y=0.4$ and could not be identified at $0.6\leqslant y$. Hence, columbite was again the sole phase detected at higher values of Nb concentration, similar to Fig. 1(a). In addition, the spectrum of $y=1.0$ (i.e., $(Mg_{0.4}Zn_{0.6})Nb_2O_6$) was also closer to that of $MgNb_2O_6$, although the $ZnNb_2O_6$ component is somewhat greater in amount in Fig. 1(b). By comparing the results of the two systems, therefore, the columbite structure turned out to be stable at high concentrations of Nb. The situation, however, was quite different at low values of x and y, due to the effect of Ta.

XRD spectra of $Pb[(Mg_{0.6}Zn_{0.4})_{1/3}(Ta_{1-x}Nb_x)_{2/3}]O_3$ (system I) and $Pb[(Mg_{0.4}Zn_{0.6})_{1/3}(Ta_{1-y}Nb_y)_{2/3}]O_3$ (system II) are compared in Fig. 2(a) and (b), respectively. In

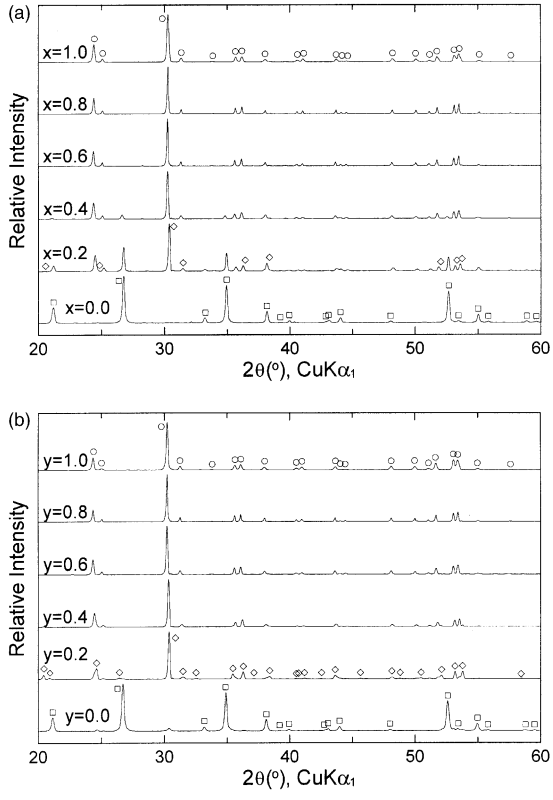

Fig. 1. XRD spectra of the B-site precursor compositions of (a) system I and (b) system II (after second calcination). (□) Trirutile, (◇) tri-αPbO_2, (○) columbite.

both systems, only a perovskite structure, together with small amounts of pyrochlore, were detected at high values of x and y. When appreciable amounts of the pyrochlore were present (e.g., $y \leqslant 0.4$ in system II), reflections of PbO ($\triangle$) and ZnO ($\triangledown$) were also observed. The two oxides are believed to be the remaining components, after pyrochlore formation from the compositions of perovskite stoichiometries. At intermediate compositions in the two systems, the perovskite contents rose gradually with increasing values of x and y at the expense of the pyrochlore. The enhancements in the perovskite formation with increasing Nb concentrations are attributed to the more-ionic nature of Nb (as compared with Ta), which favors the perovskite structure over the less-ionic pyrochlore. Meanwhile, slight shifts of the reflection angles to lower values with increasing Nb concentrations could be noticed in both systems. This behavior is directly associated with the somewhat-larger ionic size of Nb over Ta [16–19], although they were reported to be identical, 0.064 nm [20]. On the other hand, superlattice reflections (associated with the superstructure formation) could not be identified at all, indicating disordered configurations in the long-range structural arrangement among the octahedral cations.

Perovskite formation yields (after sintering), determined by comparing the major peak intensities of perovskite (110) and pyrochlore (222) reflections, are plotted in Fig. 3 for the two systems. The perovskite contents changed continuously in the ranges of 79% ($x = 0.0$) to 100% ($x = 0.8$ and 1.0) and 33% ($y = 0.0$) to 98% ($y = 1.0$) in systems I and II, respectively. The yields in system I, however, were much higher than those in system II (especially at low concentrations of Nb), implying that the additional replacements by 20 at.% Mg in system I had significantly promoted the perovskite formation.

Frequency-dependent dielectric constant spectra of representative compositions (possessing highest maximum dielectric constants) in systems I ($x = 1.0$) and II ($y = 1.0$) are displayed in Fig. 4. Values of the maximum dielectric constant and corresponding temperature of $x = 1.0$ were 23,300 (43 °C), 21,800 (47 °C), 20,200 (51 °C), and 18,200 (57 °C) at 1, 10, 100, and 1000 kHz, respectively, whereas the values of $y = 1.0$ were 20,700 (72 °C), 20,000 (75 °C), 18,700 (78 °C), and 17,100 (82 °C) at the same frequency decades. In the two compositions, diffuse modes in the phase transition, along with strong dispersion (i.e., increases in the dielectric maximum temperature and decreases in the maximum dielectric constant with increasing measurement frequency) of relaxor ferroelectrics, are well demonstrated. The dielectric spectra of other compositions in the two

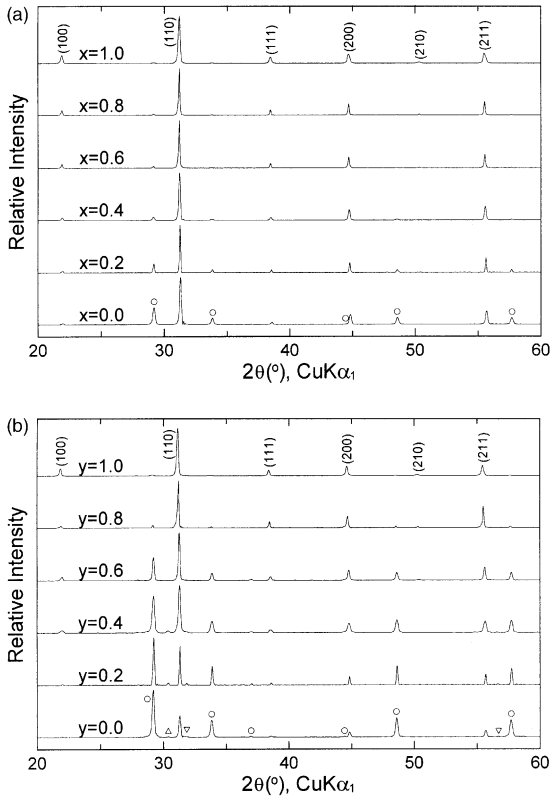

Fig. 2. X-ray diffractograms of (a) system I and (b) system II (after second calcination). (hkl) Perovskite, (○) pyrochlore, ($\triangle$) PbO, ($\triangledown$) ZnO.

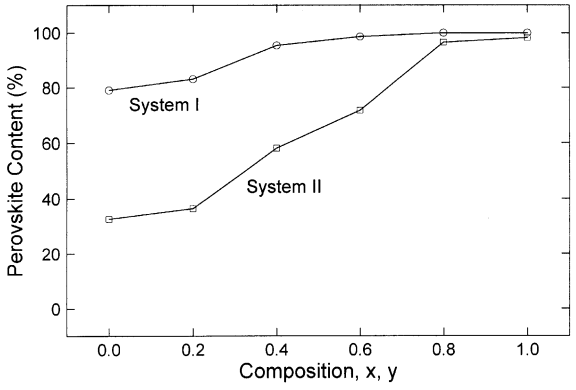

Fig. 3. Perovskite formation yields of the two system compositions.

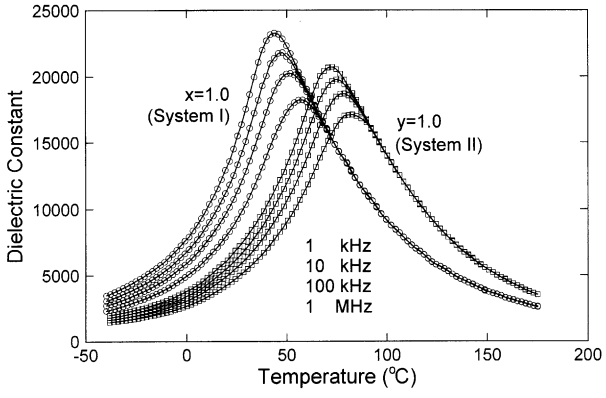

Fig. 4. Variations of the dielectric constant values of $x = 1.0$ (system I) and $y = 1.0$ (system II) with frequency change.

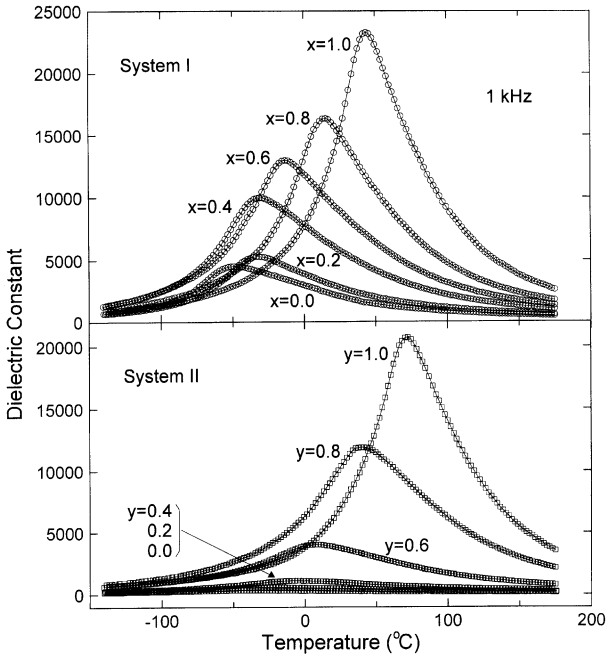

Fig. 5. Dielectric constant spectra of the whole compositions in the two systems.

systems also exhibited similar relaxation of frequency dependencies.

Variations of the dielectric constant spectra with compositional change in systems I and II are shown in Fig. 5. In both systems, the maximum dielectric constants increased with increasing values of x and y: 4500–23,300 ($x = 0.0$–1.0) and 330–20,700 ($y = 0.0$–1.0) at 1 kHz. Meanwhile, the maximum values at identical Nb concentrations in system I (60 at.% Mg) were higher than those in system II (40 at.% Mg), which can be attributed to the active role of Mg in long-range dipole interaction. In contrast, dielectric maximum temperatures in system II (−49 to 72 °C) were somewhat higher than those in System I (−50 to 43 °C), which is consistent with the higher dielectric maximum temperatures in the Zn-containing compounds, as compared with the Mg-analogs: e.g., 140 °C in $Pb(Zn_{1/3}Nb_{2/3})O_3$ [21–23] versus −10 to −5 °C in $Pb(Mg_{1/3}Nb_{2/3})O_3$ [11,15,22,24], −20 to −10 °C (extrapolated value [11]) in $Pb(Zn_{1/3}Ta_{2/3})O_3$ versus −88 to −85 °C in $Pb(Mg_{1/3}Ta_{2/3})O_3$ [14,18,25,26], etc.

4. Summary

In the B-site precursor system with 60 at.% Mg substitution, trirutile was the only structure identified at $x = 0.0$, which was immediately replaced by columbite as the major phase at $0.2 \leqslant x$. Similarly, trirutile and tri-αPbO_2 structures were predominant at $y = 0.0$ and 0.2, respectively, in the B-site precursor system with 40 at.% Mg, whereas columbite was mostly detected at $0.4 \leqslant y$. After PbO addition, in contrast, perovskite and pyrochlore structures coexisted at low values of x and y, but the perovskite formation yields rose with increasing Nb concentration: 79–100% (system I) and 33–98% (system II). In addition, the perovskite contents in system I were substantially higher than those in system II across the entire composition range. Diffuse modes in the phase transition, along with frequency-dependent dielectric relaxation, were observed at all compositions in the two systems. Furthermore, maximum dielectric constants and corresponding temperatures (@1 kHz) increased continuously with increasing Nb concentration: 4500–23,300 (−50–43 °C) and 330–20,700 (−49 to 72 °C) in systems I and II, respectively. The maximum dielectric constants in system I were higher than those in system II, whereas the reverse holds true for the dielectric maximum temperatures.

Acknowledgements

This study was supported by a grant from the Korea Research Foundation (KRF-99-041-E00528).

References

[1] J. Chen, A. Gorton, H.M. Chan, M.P. Harmer, Effect of powder purity and second phases on the dielectric properties of lead magnesium niobate ceramics, J. Am. Ceram. Soc. 69 (12) (1986) C303–C305.
[2] T.R. Shrout, A. Halliyal, Preparation of lead-based ferroelectric relaxors for capacitors, Am. Ceram. Soc. Bull. 66 (4) (1987) 704–711.
[3] P. Ravindranathan, V. Srikanth, S. Komarneni, A.S. Bhalla, Processing of $Pb(Zn_{1/3}Nb_{2/3})O_3$ ceramics at high pressures, Ferroelectrics 188 (1-4) (1996) 135–141.
[4] J. Wang, D. Wan, J. Xue, W.B. Ng, Synthesizing nanocrystalline $Pb(Zn_{1/3}Nb_{2/3})O_3$ powders from mixed oxides, J. Am. Ceram. Soc. 82 (2) (1999) 477–479.
[5] S.-E. Park, M.L. Mulvihill, P.D. Lopath, M. Ziparro, T.R. Shrout, Crystal growth and ferroelectric related properties of $(1-x)Pb(A_{1/3}Nb_{2/3})O_3 - xPbTiO_3 (A = Zn^{2+}, Mg^{2+})$, in: Proceedings of the 10th IEEE International Symposium on Applications of Ferroelectrics, 1996, pp. 79–82.
[6] C.S. Park, K.Y. Lim, D.Y. Choi, S.J. Chung, Crystal growth of $PbMg_{1/3}Nb_{2/3}O_3$ and $PbZn_{1/3}Nb_{2/3}O_3$ and structural studies on the ordering, J. Kor. Phys. Soc. 32 (Suppl.) (1998) S974–S977.
[7] B.-H. Lee, N.-K. Kim, J.-J. Kim, S.-H. Cho, Perovskite formation sequence by B-site precursor method and dielectric properties of PFW-PFN ceramics, Ferroelectrics 211 (1–4) (1998) 233–247.
[8] B.-H. Lee, N.-K. Kim, B.-O. Park, Perovskite formation and dielectric characteristics of $PFW_{0.2}$ $PFT_{0.8-x}$ PFN_x system ceramics, Ferroelectrics 227 (1-4) (1999) 87–96.
[9] H.C. Ling, M.F. Yan, W.W. Rhodes, Phase stability in $Pb(B'^{3+}_{1/2}B^{5+}_{1/2})O_3$ and $Pb(B'^{2+}_{1/3}B''^{5+}_{2/3})O_3$ compositions, Ferroelectrics 89 (1989) 69–80.
[10] S.-M. Lim, N.-K. Kim, Perovskite phase developments in $Pb[(Mg, Zn)_{1/3}Ta_{2/3}]O_3$ system and dielectric characteristics, J. Mater. Sci. 35 (17) (2000) 4373–4378.
[11] M.-C. Chae, S.-M. Lim, N.-K. Kim, Stabilization of perovskite phase and enhancement in dielectric properties by substitution of

$Pb(Mg_{1/3}Nb_{2/3})O_3$ to $Pb(Zn_{1/3}Ta_{2/3})O_3$, Ferroelectrics 242 (1-4) (2000) 25–35.
[12] B.-Y. Ahn, N.-K. Kim, Perovskite phase developments and dielectric characteristics in barium-substituted lead zinc tantalate system, Mater. Res. Bull. 35 (10) (2000) 1677–1687.
[13] S.-M. Lim, Phase Developments and Dielectric Characteristics of PMT–PZT–PZN Ceramics Prepared by B-site Precursor Method, MS thesis, Kyungpook National University, Daegu, Korea, 1999.
[14] M.-C. Chae, N.-K. Kim, J.-J. Kim, S.-H. Cho, Preparation and dielectric properties of $Pb[(Mg_{1/3}Ta_{2/3}), (Zn_{1/3}Nb_{2/3})]O_3$ relaxor ceramics, Ferroelectrics 211 (1-4) (1998) 25–39.
[15] M.-C. Chae, N.-K. Kim, J.-J. Kim, S.-H. Cho, Preparation of $Pb(Mg_{1/3}Nb_{2/3})O_3 - Pb(Zn_{1/3}Nb_{2/3})O_3$ ceramics by the B-site precursor method and dielectric characteristics, J. Mater. Sci. 33 (5) (1998) 1343–1348.
[16] F. Galasso, W. Darby, Preparation of single crystals of complex perovskite ferroelectric and semiconducting compounds, Inorg. Chem. 4 (1) (1965) 71–73.
[17] A.V. Titov, O.I. Chechernikova, Yu.N. Venevtsev, Solid solutions based on lead ferroniobate and ferrotantalate, Inorg. Mater. 14 (6) (1978) 891–894.
[18] M.-C. Chae, N.-K. Kim, Perovskite formation by B-site precursor method and dielectric characteristics of $Pb[Mg_{1/3}(Ta, Nb)_{2/3}]O_3$ ceramic system, Ferroelectrics 209 (3) (1998) 603–613.
[19] B.-Y. Ahn, N.-K. Kim, Role of B″ ion (B″ = Nb, Ta) on perovskite development, lattice parameters, and dielectric properties of $(Ba, Pb)(Zn_{1/3}B''_{2/3})O_3$ ceramics, J. Mater. Sci. 37 (21) (2002) 4697–4701.
[20] R.D. Shannon, Revised effective ionic radii and systematic studies of interatomic distances in halides and chalcogenides, Acta Cryst. A32 (5) (1976) 751–767.
[21] V.A. Bokov, I.E. Myl'nikova, Ferroelectric properties of monocrystals of new perovskite compounds, Sov. Phys.-Solid State 2 (11) (1961) 2428–2432.
[22] Y. Yamashita, Relaxor ceramic dielectric materials for multilayer ceramic capacitors, in: Proceedings of the 7th IEEE International Symposium on Applications of Ferroelectrics, 1990, pp. 241–245.
[23] Y. Yamashita, PZN-based relaxors for MLCCs, Am. Ceram. Soc. Bull. 73 (8) (1994) 74–80.
[24] D.-H. Suh, D.-H. Lee, N.-K. Kim, Phase developments and dielectric/ferroelectric responses in PMN-PT ceramic system, J. Eur. Ceram. Soc. 22 (2) (2002) 219–223.
[25] Z.G. Lu, C. Flicoteaux, G. Calvarin, Dielectric and crystallographic study of the lead magnotantalate relaxor, Mater. Res. Bull. 31 (5) (1996) 445–452.
[26] M.A. Akbas, P.K. Davies, Processing and characterization of lead magnesium tantalate ceramics, J. Mater. Res. 12 (10) (1997) 2617–2622.